Transition-matrix model of bioturbation and radionuclide diagenesis

David H. Shull[1]

Environmental, Coastal, and Ocean Sciences Department, University of Massachusetts Boston, Boston, Massachusetts 02126

Abstract

Bioturbation rates in muddy sediments are thought to be due primarily to the reworking activities of benthic deposit feeders. However, current mathematical models of bioturbation do not explicitly link rates of particle mixing with realistic biological reworking mechanisms. To address this problem, I present a transition-matrix model of bioturbation that quantitatively links the reworking activities of individual organisms and community-level particle-mixing rates. Solutions to the model are presented for two kinds of tracers; particle-reactive radionuclides with a constant input flux and conservative tracers added to the sediment as a pulse. The model was used to predict the vertical profiles of excess ^{234}Th and ^{210}Pb in the field. The model parameters were determined from benthic community-structure data. Model predictions were then compared to measured profiles of these tracers. On the basis of this comparison, I inferred that maldanid polychaetes at the study site were collecting sediment at the sediment-water interface and depositing it at depth. This transport mechanism had a large effect on the predicted tracer profiles. A sensitivity analysis of the model indicated that deposit feeding by the two most abundant species, *Mediomastus ambiseta* and *Nucula annulata,* was the most important process determining the burial rate of the tracers. The model results also indicated that the combined effects of deposit feeding and sedimentation were sufficient to determine the vertical distributions of excess ^{234}Th and ^{210}Pb at the study site.

The muddy sea floor is an environment of complex and vigorous activity. Organisms representing many taxa construct pits, mounds, tubes, pellets, and burrows. Deposit-feeding benthos use assorted tentacles, appendages, and mouthparts to consume and rework various components of the sediment, often at remarkably rapid rates (*reviewed by* Thayer 1983). Many species irrigate their dwellings by swiftly beating appendages, by peristaltic movements, or by oscillating like pistons in their tubes. These activities, termed ''bioturbation,'' have well-documented, dramatic effects on many important sea-floor properties, including sediment geochemistry, stratigraphy, microbial activity, benthic community ecology and evolution, and contaminant transport (*reviewed by* Berner 1980; Aller 1982; Olsen et al. 1982; Lopez et al. 1989; Boudreau 1997). It is important to accurately quantify the rates and mechanisms of bioturbation in order

to understand the effects of benthic organisms on these processes.

In the narrowest sense, bioturbation refers to the displacement and mixing of sediment particles due to the activities of organisms (Richter 1952). Two approaches have been taken to quantify rates of particle bioturbation. Reworking rates of individual organisms have been directly measured in the laboratory. Alternatively, rates of particle mixing have been calculated from profiles of particulate tracers in the field.

Bioturbation rates from laboratory studies have resulted in a wealth of data on the particle-reworking rates (mass sediment per individual per time) of many benthic species (*reviewed by* Cammen 1980; Thayer 1983). These studies have also identified many different mechanisms by which organisms transport particles. In this paper, I will refer to these mechanisms using the following simple classifications, based on the directions of particle movement. The collection of particles at depth and their deposition at the sediment-water interface will be termed ''upward transport.'' (This kind of transport is also known as ''conveyor-belt feeding.'') I will term the collection of particles at the sediment surface and their deposition at depth ''downward transport.'' The collection and deposition of particles at depth will be called ''interior transport.'' Finally, ''surface transport'' will refer to the collection and deposition of particles at the sediment surface.

The other approach for quantifying particle-mixing rates is the measurement of particulate tracer profiles. These tracers include the excess activity of particle-reactive radionuclides scavenged from the water column and deposited at the sediment surface, such as ^{234}Th or ^{210}Pb (Aller and Cochran 1976; Nozaki et al. 1977), the concentration chlorophyll *a* (Sun et al. 1991), artificial particles such as glass beads, fluorescent spheres, or brightly colored plastic fragments usually deposited on the sediment surface as a pulse (Wheatcroft 1991, 1992; Gerino et al. 1998), isotopically labeled

algae or sediment labeled with rare-earth elements (Levin et al. 1997; Wheatcroft et al. 1994), and conspicuous particles deposited by a natural process at a known time in the past (Guinasso and Schink 1975). The particle-mixing rate is then determined by comparing a measured tracer profile with one predicted by a mathematical model. The mixing rate is calculated as the value of a model parameter that provides the best statistical fit of the model to the measured tracer profile (e.g., Officer and Lynch 1983).

When the tracer approach is used, particle mixing has been traditionally modeled under the assumption that the mixing mechanism is analogous to diffusion (Goldberg and Koide 1962). This means that the ensemble of particle-reworking activities can be modeled as though it were a large number of small, random, particle displacements. Alternatively, particle mixing has been modeled as a bioadvective velocity (Rice 1986; Robbins 1986). In this formulation, particle reworking consists of upward transport, where particles are collected at the bottom of the mixed layer and deposited at the sediment surface. The bioadvective velocity is the result of the subsequent downward gravitative movement of particles in the sediment column as subsurface voids, created by the removal subsurface sediment, are filled with sediment from above.

When tracer profiles cannot be adequately reproduced by bioadvection or biodiffusion models, more complex models, termed ''nonlocal'' models, have been used. These models allow sediment to be collected and deposited at various depths in the sediment (e.g., Smith et al. 1986; Boudreau and Imboden 1987; Pope et al. 1996). Nonlocal models can provide better fits to tracer profiles that exhibit complex patterns, such as subsurface maxima. However, in a series of papers, Boudreau demonstrated that vastly different particle-mixing mechanisms could produce nearly identical tracer profiles (Boudreau 1986a,b; Boudreau and Imboden 1987). Thus, tracer profiles alone may not provide enough information to determine the particle-mixing mechanisms occurring at a particular location.

In order to accurately model bioturbation in communities possessing complex particle-reworking mechanisms, I present a discrete mathematical model that quantitatively links laboratory observations of particle mixing by individual organisms and the community-level mixing processes that determine tracer profiles in the field. The model can predict tracer distributions, given data on the composition of benthic communities. Thus, the model can be tested by comparing predicted and measured tracer distributions. Because benthic biological data and geochemical data are often discrete with respect to depth, this discrete model is a useful interface between measured biological and geochemical processes. After describing the model, I will use data on benthic community structure collected from a site in Narragansett Bay along with literature values of organism feeding rates and mechanisms determined in the laboratory to predict the profiles of two radionuclide tracers of bioturbation, ^{234}Th and ^{210}Pb. Differences between measured and predicted profiles suggest that some species that traditionally have been considered ''conveyor-belt species'' are collecting a significant percentage of sediment from the sediment-water interface and depositing these particles at depth.
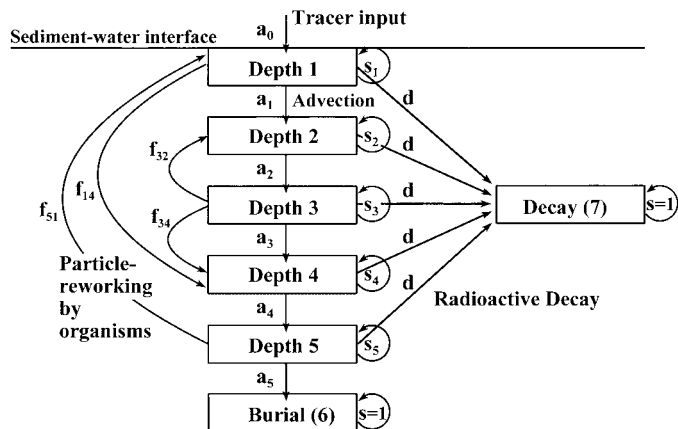

Fig. 1. Diagrammatic representation of the transition-matrix bioturbation model. Boxes represent different model states: depths in the sediment column, burial, or radioactive decay. Arrows represent hypothetical tracer-particle trajectories. Tracer movement is determined by the nondimensional variables, f, a, s, and d, which correspond to locations in the transition matrix of Fig. 2. These variables represent the transition probabilities or, equivalently, the fraction of tracer in each state that moves to another state in one model time step.

Transition-matrix particle-mixing model

The sediment is envisaged as a series of discrete boxes of thickness Δx (Fig. 1). The five depth boxes, or states, in Fig. 1 represent stratigraphic layers in the sediment, whereas the burial state represents permanent removal from the mixed layer. The state labeled ''decay'' represents the loss of a radioactive tracer due to radioactive decay. The arrows represent particle (or tracer) trajectories. The rates of movement among states are determined by transition probabilities. The transition probabilities are equivalent to the fraction of sediment moved from one box to another in one time step. The transition probabilities f_{ij} in Fig. 1 represent the movement of particles due to the activities of organisms. Just 4 of the 20 possible trajectories are shown (f_{51}, f_{14}, f_{32}, and f_{34}). The advection terms, a_i, represent the subsequent downward movement of particles in the sediment column as voids at depth are filled. In each box, d is the fraction of tracer undergoing radioactive decay. Finally, s_i represents the fraction of particles in each box that does not move to another state. These processes can be quantified by use of a transition matrix, P (Fig. 2).

Creating a simple, one-dimensional model that directly relates particle-mixing rates to the reworking activities of macrofauna requires the following assumptions. Some of these assumptions may be relaxed to model more complex processes. All mixing is assumed to be due to the particle-reworking activities of macrofauna. (It will be assumed later that all particle mixing is due to the reworking activities of deposit feeders.) Only vertical mixing processes are considered. The transition probabilities are assumed to be time invariant. With these assumptions, the transition matrix can be conveniently analyzed by use of Markov-chain theory (Kemeny and Snell 1976). Markov-chain theory provides simple

State at time t ↓	State at time t + 1						
	1	2	3	4	5	Burial	Decay
1	s_1	$a_1(1\text{-}d)$	0	$f_{14}(1\text{-}d)$	0	0	d
2	0	s_2	$a_2(1\text{-}d)$	0	0	0	d
3	0	$f_{32}(1\text{-}d)$	s_3	$a_3(1\text{-}d)+f_{34}(1\text{-}d)$	0	0	d
4	0	0	0	s_4	$a_4(1\text{-}d)$	0	d
5	$f_{51}(1\text{-}d)$	0	0	0	s_5	$a_5(1\text{-}d)$	d
Burial	0	0	0	0	0	1	0
Decay	0	0	0	0	0	0	1

Fig. 2. Transition matrix. Elements of the transition matrix determine the rates of movement from state to state in the model. The elements of the main diagonal represent the fraction of tracer not moving each time step. The fraction of tracer remaining in the burial and decay states equals 1, because burial and radioactive decay permanently remove tracer from the rest of the system.

analytical solutions to the model for a variety of initial or boundary conditions.

The elements of the transition matrix that determine the rates of particle mixing can be directly related to the sediment-reworking rates of organisms. Let b_{ij} be the rate (mg particle time^{-1}) at which organisms collect particles at depth i and deposit the particles at depth j. For boxes of unit area, the box volume (cm^3 wet sediment) is Δx. The fraction of material moved from one state to another in one model time step, Δt, is

$$f_{ij} = \frac{b_{ij}\Delta t}{\Delta x \rho (1 - \varphi)} \tag{1}$$

where φ is the sediment porosity (cm^3 porewater cm^{-3} wet sediment) and ρ is the solids density (mg particle cm^{-3} particle), so that $\rho (1 - \varphi)$ has units mg particle cm^{-3} wet sediment.

Movement of particles within the sediment column and sedimentation of particles from the water column result in the burial of sediment by advection. During burial, sediment is compacted as porewater is squeezed out. These processes are included in the advection term, a_i.

$$a_i = a_{i-1}\frac{(1 - \varphi_{i-1})}{(1 - \varphi_i)} + \frac{\sum_{j=1}^{m} f_{ji}(1 - \varphi_j)}{(1 - \varphi_i)} - \sum_{j=1}^{m} f_{ij}, \tag{2}$$

where m is the number of depth strata in the model. This equation represents a mass balance. Porosity is allowed to vary among depths. The first term on the right side of the equation represents the amount of tracer entering depth i from depth $i - 1$ (the depth just above it in the sediment column) due to advection. The next term represents tracer entering depth i from all other depths, j, due to the sediment-reworking activities of organisms. The final term represents the movement of tracer from depth i to all other depths, j, due to the reworking activities of organisms. At the sediment-water interface ($i = 1$), a_1 is the sum of net particle deposition due to sediment reworking and deposition of sediment from the water column (i.e., $a_0 = s\Delta t \Delta x^{-1}$, where s is the sedimentation rate). The advection terms along the upper

off diagonal of the transition matrix are appropriate for the conditions of net deposition. Including similar terms along the lower off diagonal could simulate net erosion. As was indicated by Boudreau (1986*b*), any discrete model of bioturbation must possess some form of Eq. 2 to insure that mass is conserved. Equation 2 is essentially a discrete form of Boudreau's (1997) solids conservation equation (Table 1).

Rates of chemical reactions can also be included in the model. One of the simplest chemical reactions to quantify is radioactive decay. The probability of a tracer undergoing radioactive decay in time Δt is

$$d = 1 - e^{-\lambda \Delta t}, \tag{3}$$

where λ is the decay coefficient for the radionuclide of interest. To convert the fraction of particles moved by feeding and advection, f_{ij} and a_i, to the fraction of tracer moved, these matrix elements are multiplied by $(1 - d)$, the fraction of tracer not undergoing radioactive decay in one model time step Δt (Fig. 2).

The fraction of tracer remaining at a particular state, s_i, is $1 - p_{i+}$, where p_{i+} denotes the sum of the ith row of the transition matrix P. The fraction of tracer remaining in the states labeled "burial" and "decay" after each time step is 1 (Fig. 2). These states are called "absorbing states," because, once tracer is buried or undergoes radioactive decay, it is lost from the rest of the system (Kemeny and Snell 1976). The remaining states, representing layers of sediment, are nonabsorbing states.

The transition-matrix model has simple solutions. The concentration profile of a tracer at any time (units, mass tracer cm^{-3} wet sediment) can be calculated by use of the transition matrix P. Given an initial tracer profile, C_0,

$$C_t = C_0 P^t, \tag{4}$$

where C_t and C_0 are row vectors containing the concentration of tracer at each depth. Given a steady flux of tracer to the sediment surface, the steady-state concentration profile, C_s, can be calculated from the equation

$$C_s = \zeta(I - Q)^{-1}, \tag{5}$$

where ζ is a row vector containing the flux of tracer to each

Table 1. Derivation of Eq. 2 from Boudreau's (1997) equation for conservation of solids.

Eq. 3.122 (Boudreau 1997):

$$\frac{\partial(1 - \varphi)B}{\partial t} = -\frac{\partial(1 - \varphi)wB}{\partial x} + \sum R_B$$

$$+ \int_0^L K(x', x; t)[1 - \varphi(x')]B(x)\ dx'$$

$$- [1 - \varphi(x)]B(x) \int_0^L K(x, x'; t)\ dx'$$

Eq. 3.122 solved for total solids, assuming porosity profile is time invariant:

$$0 = -\frac{\partial(1 - \varphi)w}{\partial x} + \int_0^L K(x', x; t)[1 - \varphi(x')]\ dx'$$

$$- [1 - \varphi(x)] \int_0^L K(x, x'; t)\ dx'$$

Backward-difference approximation for advection, approximating the integrals as summations. E_{ij} is the exchange rate (units, time^{-1}) among depths i and j:

$$0 = -\frac{w_i(1 - \varphi_i) - w_{i-1}(1 - \varphi_{i-1})}{\Delta x} + \sum_{j=1}^m E_{ji}(1 - \varphi_j)$$

$$- (1 - \varphi_i) \sum_{j=1}^m E_{ij}$$

Multiplying by Δt, dividing by $(1 - \varphi_i)$, letting $f_{ij} = \Delta t E_{ij}$ and $a_i = w_i \Delta t \Delta x^{-1}$:

$$a_i = a_{i-1}\frac{(1 - \varphi_{i-1})}{(1 - \varphi_i)} + \frac{\sum_{i=1}^m f_{ji}(1 - \varphi_j)}{(1 - \varphi_i)} - \sum_{j=1}^m f_{ij}$$

---

depth (units, mass area^{-1} time^{-1} cm^{-1}), I is the identity matrix, and Q is the submatrix of nonabsorbing states (Roberts 1976). The matrix $(I - Q)^{-1}$, termed the "fundamental matrix" (Kemeny and Snell 1976), represents the residence time of a tracer at each depth. By setting the decay probability to 0, Eq. 4 can be used to model the distribution of a conservative tracer added to the sediment as a pulse. Equation 5 can be used to model the steady-state distribution of a tracer with a constant input flux, such as the excess activity of radionuclides.

Transition matrix sensitivity analysis

A transition matrix with two absorbing states will contain two eigenvalues equal to 1 (Roberts 1976). The third largest eigenvalue is a measure of the rate of burial (or decay) of a tracer in the sediment. The change in the third largest eigenvalue for a given change in each matrix element ($\partial \lambda_3/\partial p_{ij}$) provides a sensitivity measurement. It determines the relative change in burial rate for a given change in a matrix element. The proportional change in λ_3 for a given change in the value of a matrix element is called the elasticity. The

elasticities for the third largest eigenvalue can be calculated as follows:

$$E_{i,j} = \frac{p_{ij}}{\lambda_3} \frac{U_3 V_3}{\langle U_3 V_3 \rangle}, \tag{6}$$

where E is the elasticity matrix with elements e_{ij}, equal to $(p_{ij}/\lambda_3)(\partial \lambda_3/\partial p_{ij})$. The vector U_3 is the left eigenvector associated with the third largest eigenvalue, V_3 is the right eigenvector, and $\langle U_3 V_3 \rangle$ is the scalar product of the left and right eigenvector matrices (Caswell 1978, 1989). Because the elements of E correspond to the rate of movement of particles due to the activities of organisms collecting particles from a particular depth, the matrix elements with the highest elasticities will indicate which groups of organisms collecting particles at a particular depth contribute most to tracer burial.

Methods

Sampling methods—I collected and analyzed samples for benthic fauna, sediment porosity, and organic carbon content to estimate the parameters of the model. Samples to be analyzed for radionuclides (^{234}Th and ^{210}Pb) were also collected so that predicted radionuclide profiles could be compared with measured profiles from the same location.

Divers collected sediment samples from Narragansett Bay (41°34′N, 71°21.5′W) at a depth of 13 m on 23 August 1997. This site was chosen because data on the spatial distribution of one of the most abundant deposit feeders (*Mediomastus ambiseta*) was known, and I expected to find measurable inventories of radionuclide tracers because of the presence of fine-grained sediments (Hughes 1996). Historical data on infaunal abundances and depth distributions from the adjacent study site of McCaffrey et al. (1980) and Grassle et al. (1985) were also available. These data indicate little year-to-year variation in benthic community structure. The historical data also indicate that a similar infaunal community has persisted here for more than two decades.

Divers collected samples of macrofauna using four small (5.5-cm inner diameter, 30-cm length) and three large (14.5-cm inner diameter, 60-cm length) cylindrical butyrate cores. The small cores were used to determine the vertical distribution of small macrofauna at the study site. Cores were stored in the dark on ice until they were returned to shore. Within 2 h after collection, these cores were sectioned at 0.5-cm intervals to 1 cm, 1-cm intervals to 10 cm, and 2-cm intervals to the bottom of the core. Sections were immediately fixed in 10% buffered formalin. Large cores were collected in order to sample less-abundant larger organisms. These cores were maintained in the laboratory with oxygenated seawater for 1 d. Afterward, one core was imaged by use of a CT scanner (Omni 4001) to determine the vertical distribution of the large infauna. The cores were then wet sieved through 1-mm mesh with use of filtered seawater. Retained animals were fixed in 10% buffered formalin.

After formalin fixation, the small-core faunal samples were washed over a 250-μm sieve, transferred to 70% ethanol, and stained with rose bengal. Large-core faunal samples were washed over a 1-mm sieve, transferred to 70%

Table 2. Abundance and modeled feeding mechanisms of deposit feeders inhabiting the Narragansett Bay study site. Standard deviations are shown in parentheses. The feeding mechanisms and rates are those used in the transition-matrix model. U = upward transport; D = downward transport; I = interior transport. Depths of particle ingestion are also given in parentheses. For some species, feeding rates were calculated from individual dry weights by use of Cammen's (1980) empirical model. For these species, the average feeding rates and standard deviations (in parentheses) are given. The standard deviations indicate the variability in calculated ingestion rates for each species due to variation in body size. The number and sizes of organisms in each core at each depth are tabulated in Shull (2000).

Deposit-feeding species	Abundance (No. 23.8 cm^{-2})	Modeled feeding mechanism (depth)	Deposit-feeding rate (mg day^{-1})	Reference (for feeding rates)
Nucula annulata	48 (20, $n = 4$)	U (1–3 cm)	6	Lopez and Cheng (1983)
Mediomastus ambiseta	32 (42, $n = 4$)	U (1–3 cm)	2.5	Wheatcroft et al. (1998)
Oligochaetes	8.5 (2.4, $n = 4$)	I (3–4 cm)	0.29 (0.13, $n = 4$)	Cammen (1980)
Sabaco elongatus	0.48 (0.22, $n = 3$)	U (15 cm)	94 (52, $n = 10$)	Cammen (1980)
Polycirrus eximius	0.29 (0.38, $n = 3$)	D (surface)	62 (27, $n = 6$)	Cammen (1980)
Macroclymene zonalis	0.24 (0.3, $n = 3$)	U (15 cm)	29 (27, $n = 5$)	Cammen (1980)
Yoldia limatula	0.05 (0.08, $n = 3$)	U (2–3 cm)	1,200	Bender and Davis (1984)

ethanol, and stained with rose bengal. All macrofauna were sorted from these samples under a dissecting microscope. Organisms were identified to species and enumerated, and their lengths were measured by means of an ocular micrometer. Lengths of larger organisms were measured with a ruler. The lengths of tubes of larger species were also measured. Body weights of deposit feeders were measured after drying in an oven at 70°C.

Samples to be analyzed for radionuclides and organic carbon were collected by use of two cylindrical 8.7-cm diameter, 40-cm long butyrate cores. These cores were sectioned at 0.5-cm intervals to 2 cm and 1-cm intervals to 6 cm. One of the cores (the one containing the longer sediment column) was also sectioned at 1-cm intervals to 29 cm. During sectioning, ~3–5 mm of sediment around the perimeter of each section was trimmed, to prevent contamination from potential smearing of sediment along the inner core wall. The remaining sample from each section was placed into a pre-weighed plastic jar. I analyzed sediment from the longer core for excess ^{210}Pb and organic carbon content. Sediment from the shorter core was analyzed for excess ^{234}Th.

Sediment chemistry—Samples to be analyzed for radionuclides were weighed wet, dried at 70°C for 24 h, and reweighed to determine sediment porosity. Samples were then ground to a powder. Eight grams of sample were transferred to preweighed plastic vials. The height of sediment in each vial was adjusted by tapping to achieve uniform geometry among all samples.

The activities of ^{234}Th and ^{210}Pb were measured with a Princeton Gamma-Tech intrinsic germanium gamma spectrometer with a well detector (model IGW-10023). The ^{234}Th activity was measured at the 63.3 keV energy peak, and ^{210}Pb activity was measured at the 46.5 keV energy peak. Counts were corrected for background. Counting efficiencies were determined by counting a U.S. Environmental Protection Agency–certified uraninite standard with all ^{238}U daughters in secular equilibrium. The standard was uniformly distributed within a matrix of powdered sediment from the study site. The weight and geometry of the standard was identical to that of the samples. Supported levels of ^{234}Th were measured at the 63.3 keV energy peak after ^{234}Th was allowed

to reach secular equilibrium with its parent, ^{238}U. Supported levels of ^{210}Pb were determined by measuring the activity of ^{214}Pb at the 352 keV energy peak. Total analytical error was determined by propagating errors associated with counting, background, and detector efficiency. Activities and analytical errors were corrected for radioactive decay occurring between the times of sample collection and counting.

The organic carbon content of dried and powdered sediment samples was determined by use of a Perkin-Elmer model 2400 CHN elemental analyzer. Prior to combustion, inorganic carbon was eliminated by adding 1 M HCl to each sample according to the wet-acidification procedure of Hedges and Stern (1984). The organic matter content of the sediment was estimated as twice the organic carbon content (Christman and Gjessing 1983).

Aluminum concentration of sediment samples was determined by atomic absorption spectrophotometry. Small portions (20 mg) of sediment were first dissolved with 5 ml aqua regia and 2 ml HF by use of microwave digestion. Samples were diluted with 1.5% H_3BO_3 and reheated in the microwave, following the procedure of Lamothe et al. (1986). Samples were further diluted with 0.1 M HNO_3. Aluminum content was determined by use of a Perkin-Elmer Zeeman 5000 Atomic Absorption Spectrophotometer and ASA 400 graphite furnace with Zeeman background correction.

Determination of model parameters by use of field data— To relate benthic community structure to particle-mixing rates in Narragansett Bay, I assumed that all particle mixing was due to deposit feeding. Although it is likely that other particle-mixing mechanisms occurred at the study site, I made this assumption to test whether rates of particle mixing by deposit feeders were sufficient to determine excess ^{234}Th and ^{210}Pb profiles in the field. Given this assumption, the rates of particle movement were determined by estimating deposit-feeding rates for each sampled organism. For some species, individuals were assigned feeding rates on the basis of laboratory studies (Table 2). For other species, the deposit-feeding rate was calculated from organism dry weight and sediment organic matter content by use of the empirical

formula of Cammen (1980). When this formula was used, deposit feeding rates, b_{ij}, were calculated as

$$b_{ij} = \sum_k 0.435 w_k^{0.771} om_i^{-0.92}, \qquad (7)$$

where w_k is the dry weight of the kth individual collecting particles at depth i and depositing them at depth j, and om_i is the fraction organic matter at depth i. The coefficients in this formula have the following 95% confidence limits: $10^{(-.36 \pm 0.2)}$, 0.771 ± 0.12, and -0.92 ± 0.2. The feeding rates of all deposit feeders sampled were used to calculate b_{ij}, which were then used to calculate the transition probabilities by use of Eq. 1. Feeding rates were corrected for the effects of temperature under the assumption of a Q_{10} of 2 (Dobbs 1981). A Q_{10} of 2 means that the modeled feeding rate doubles for each 10° increase in temperature. The ambient temperature was used to predict the excess ^{234}Th profile. For the excess ^{210}Pb profile, the yearly average temperature at the study site was used for determining feeding rates (Kremer and Nixon 1978). The sedimentation rate (calculated from the excess ^{210}Pb profile between 15 and 25 cm) was 1.5 mm yr^{-1}.

Although maldanid polychaetes are conveyor-belt species, they are also known to collect material from the sediment surface by a process called ''hoeing'' (Dobbs and Whitlatch 1982; Levin et al. 1997). However, the hoeing rates for the species collected at the study site were unknown. Therefore, the transition-matrix model was initially run under the assumption that the maldanids collected no sediment from the sediment surface. Then the fraction of ingested sediment collected at the sediment surface was varied, and the model was rerun to determine the best fit to the ^{210}Pb profile (the fit that minimized the residual sum of squares). In this manner, the hoeing rate of the maldanid polychaetes was estimated from the tracer profile. However, the other model parameters were determined independently of the tracer profiles.

The vertical distributions of the more abundant species were determined from their occurrence in the vertically sectioned small-diameter cores. The vertical distributions of the larger, relatively rare species were determined from published data and direct observations. For the maldanid polychaetes, x-radiographs collected from the same site by McCaffrey et al. (1980) indicated a feeding depth of 15 cm. The computer tomography images of the large core showed three maldanid feeding voids with a mean depth of 15.3 cm (1.2 cm SD). For the terrebellid polychaete *Polycirrus eximius,* the observations of Myers (1977) and Starczak et al. (pers. comm.) indicated that these organisms collect sediment at the sediment-water interface and deposit it at a depth of ~3 cm (Starczak pers. comm.). The modeled depth distributions of the maldanid and terrebellid polychaetes were normally distributed around the mean feeding depth. The modeled depth distribution of maldanid-polychaete feeding had a mean of 15 cm (1 cm SD). The modeled depth distribution of *P. eximius* sediment egestion had a mean of 3 cm (0.25 SD). The modeled depth distribution of the feeding appendages of *Yoldia limatula* was uniform from 1 to 2 cm (Bender and Davis 1984). For *P. eximius* to deposit sediment at depth within its tube, it was assumed that this species

created a burrow large enough to accommodate the egested sediment and discarded the excavated material at the sediment surface. Thus, the rate of upward transport due to burrow construction was equal to the rate of downward transport due to deposit feeding.

To predict the steady-state profiles of radionuclide tracers by use of Eq. 5, the flux of the tracer to the sediment surface must be determined. Fluxes of excess ^{234}Th and ^{210}Pb were determined from the measured inventory of these radionuclides. This value was then used for the flux term in Eq. 5, so that predicted and measured tracer profiles could be compared in one plot.

The appropriate time step (Δt) and box size (Δx) of the model were determined by experiment. Because tracer in each box is mixed instantly, a large Δx would artificially inflate the mixing rate. On the other hand, since the model does not allow for multiple transitions during the period Δt, a large Δt would result in an artificially slow mixing rate. The model was run with successively smaller values of Δx and Δt until the predicted profile no longer changed with decreasing Δx and Δt (determined by calculating the residual sum of squares for different values of Δx and Δt). Subsequent simulations were run with Δx set at 2 mm and Δt set at 1 d. Since the modeled depth intervals were smaller than the 0.5-cm and 1-cm depth intervals of the faunal samples, it was assumed that organisms were uniformly distributed within each depth section. Faunal abundances were then calculated at 2-mm (Δx) intervals. The porosity and organic matter content of the sediment were estimated at each model depth by cubic spline interpolation of the porosity and organic matter concentration profiles.

Results

Benthic community composition—The composition of the benthic community at the Narragansett Bay study site is summarized in Table 2 and Fig. 3. The most abundant organism at the study site was the bivalve *Nucula annulata.* The second most abundant species was the polychaete *M. ambiseta.* These species inhabited the top 2–3 cm of the sediment. They collect sediment primarily at 2- to 3-cm depth and deposit this material at the sediment surface. Also abundant were oligochaetes that were found at depths between 3 and 4 cm. It was assumed that these organisms transported particles one body length vertically within the sediment column. The polychaete *P. eximius* was also present. This species has been observed to collect particles at the sediment surface and deposit them at the base of their tubes at a depth of ~3 cm (Myers 1977; Starczak pers. comm.). The conveyor-belt feeder *Y. limatula* was also found at the site. The deepest dwelling species were the conveyorbelt feeding maldanid polychaetes *Sabaco elongatus* and *Macroclymene zonalis.*

Sediment physical and chemical properties—The model required data on sediment porosity and organic matter content. Porosity varied from 63% near the sediment surface to ~56% at depth. There was a subsurface peak in porosity at 15 cm, near the feeding depth of the maldanid polychaetes (Fig. 4A, Table 2), and another peak at 25 cm, although it
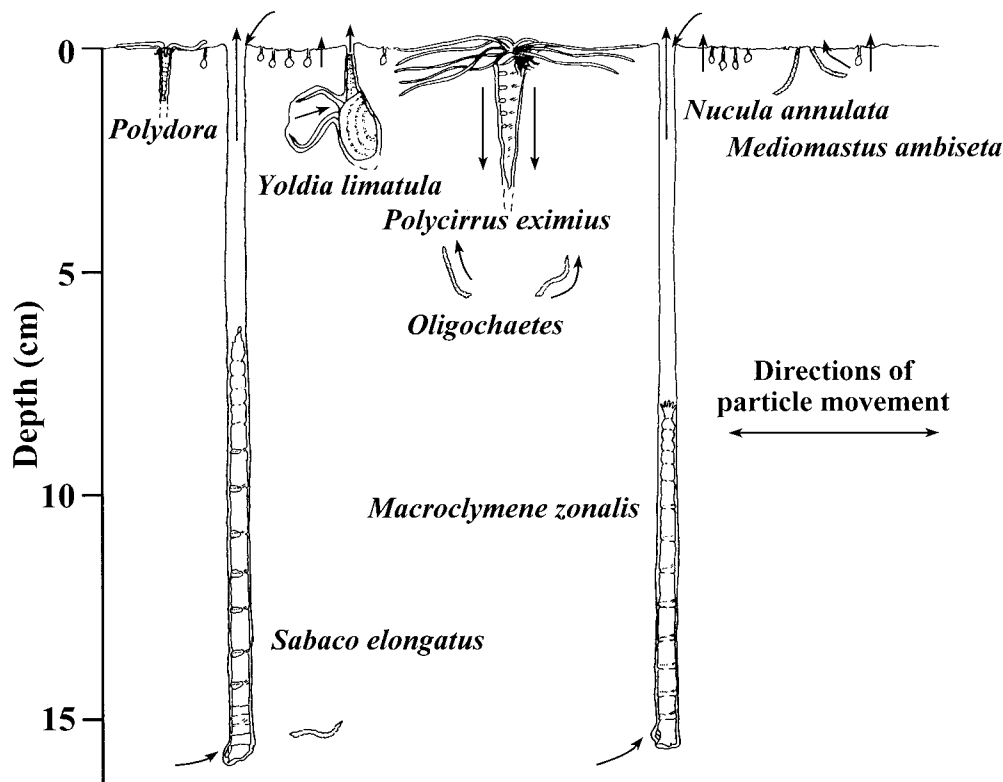
Fig. 3. The most abundant deposit feeders sampled at the Narragansett Bay study site. Arrows indicate particle trajectories. Feeding mechanisms and rates are summarized in Table 2.

is not possible to distinguish these features from random variation. The organic carbon content of the sediment varied from 1.2% near the sediment surface to ~0.9% at depth (Fig. 4B). The organic carbon:aluminum molar ratio (OC:Al) steadily decreased with depth to 23 cm. However, there was a small subsurface peak in OC:Al at 15 cm and an increase in the ratio below 25 cm (Fig. 4C).

Sediment mixing rates and mechanisms—Whereas particles were collected from a variety of depths, most particles were deposited at the sediment surface (Fig. 5). Only *Polycirrus* egested particles at depth. The modeled egestion depth for this species was 3 cm. On average, 97% of sediment collected by deposit feeders was deposited at the sediment surface (when the maldanid polychaetes were not al-

lowed to hoe surface sediment). Only 3% was egested at depth.

The measured profile of excess ^{210}Pb showed a well-mixed layer to 5 cm (Fig. 6A). The profile had a steeper slope from 5 to ~13 cm. It also showed a pronounced subsurface maximum at 15 cm. The profile predicted by the model without hoeing did not match the measured profile. There was no subsurface maximum (Fig. 6A). However, when the maldanid polychaetes were allowed to collect 40% of ingested sediment from the sediment surface, the model profiles matched the measured ^{210}Pb profiles reasonably well (Fig. 6B).

The measured profile of excess ^{234}Th activity showed a maximum at the sediment surface and decreased with depth (Fig. 7). There was a subsurface maximum at 3 cm. The excess ^{234}Th profile predicted by the transition-matrix model
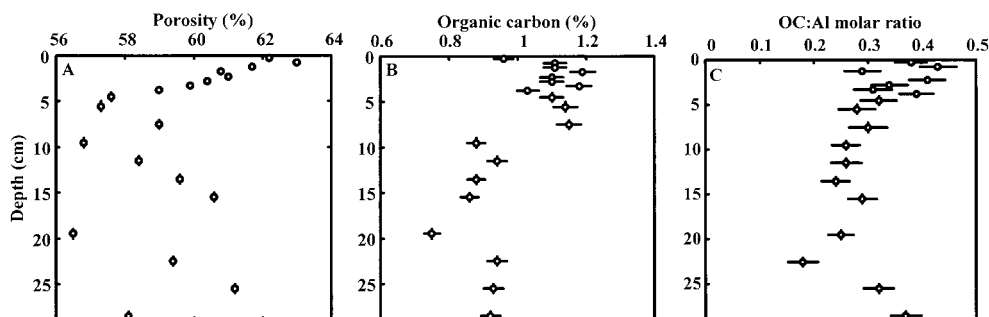

Fig. 4. Sediment properties: (A) sediment porosity, (B) sediment organic carbon profile, and (C) OC:Al. Horizontal error bars represent analytical error (± 1 SD).
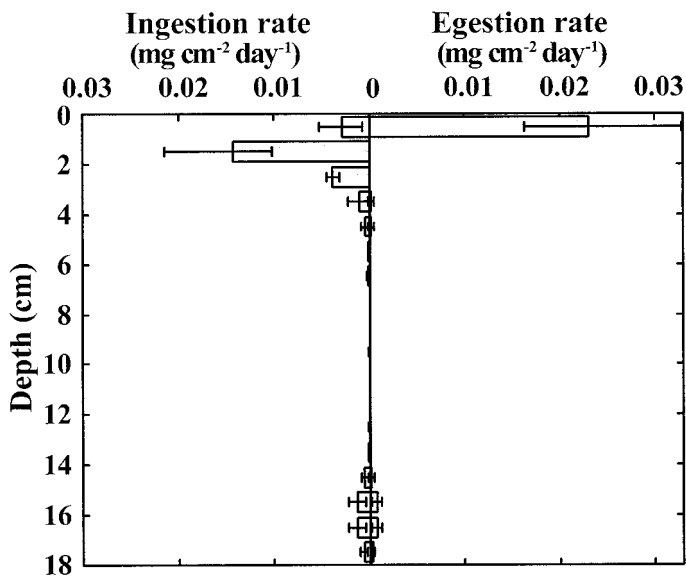
Fig. 5. Rates and depths of particle movement at the study site. Ingestion rates at each depth represent the sum of all deposit feeding rates in each row of the transition matrix ($f_{i,+}$), whereas egestion rates represent the sum of deposit-feeding rates in each column of the transition matrix ($f_{+,j}$). For this plot, the model box size (Δx) was set at 1 cm. Error bars represent the range in ingestion and egestion rates at each depth.

closely matched the measured profile down to a depth of 2 cm. It also showed a subsurface maximum in the same region as the measured maximum. This modeled subsurface maximum was due to the subsurface egestion of surface sediment by *P. eximius*.

Elasticity analysis—The results of the sensitivity analysis were contained in the elasticity matrix (Eq. 6). The elasticity
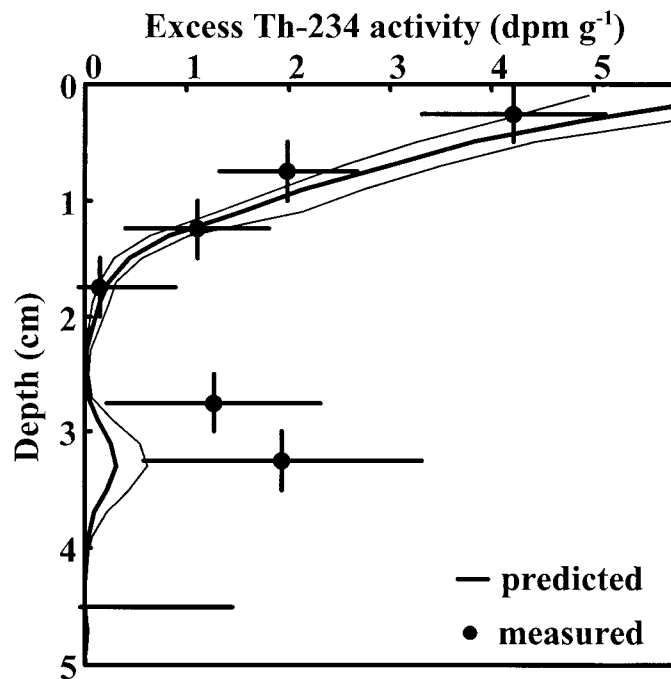

Fig. 7. Predicted and measured profiles of ^{234}Th. Bold, solid line represents the predicted mean of excess ^{234}Th activity. Finer lines represent the range of excess ^{234}Th activity, given spatial variability in benthic community structure. Solid circles represent measured excess ^{234}Th activity. Horizontal error bars represent total analytical error (± 1 SD).

matrix was large, possessing ~10,000 elements. However, it is summarized as a diagram in Fig. 8. The matrix elements with the largest elasticities were associated with particles collected at a depth of 2–3 cm and deposited at the sediment surface. The next largest elasticities were associated with the collection of particles from a depth of 14–15 cm with de-
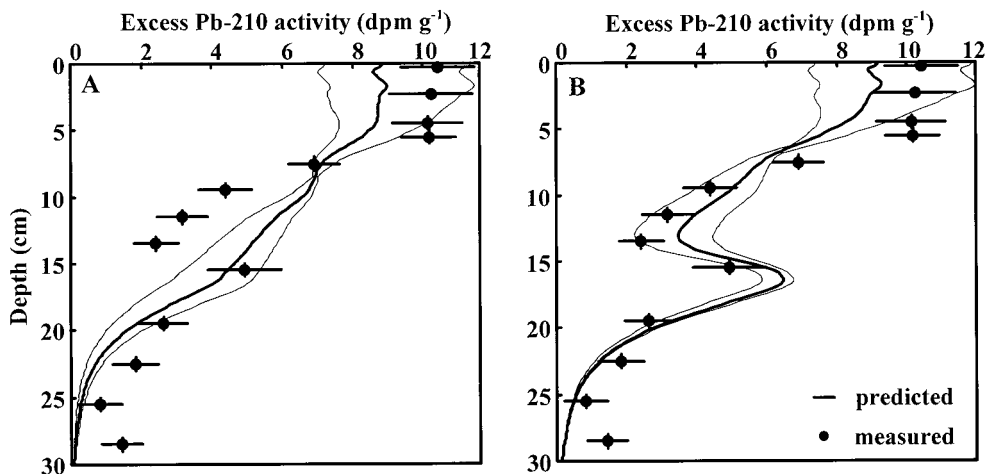

Fig. 6. (A) Predicted and measured profiles of ^{210}Pb without hoeing activity. Solid lines represent the predicted mean and range of excess ^{210}Pb activity, given spatial variability in benthic community structure. Solid circles represent the measured excess ^{210}Pb activity. Horizontal error bars represent total analytical error (± 1 SD). (B) Predicted and measured profiles of ^{210}Pb with maldanid polychaetes hoeing sediment to the bottom of their burrows. In this simulation, 40% of sediment ingested by maldanid polychaetes consisted of material collected at the sediment surface by hoeing.
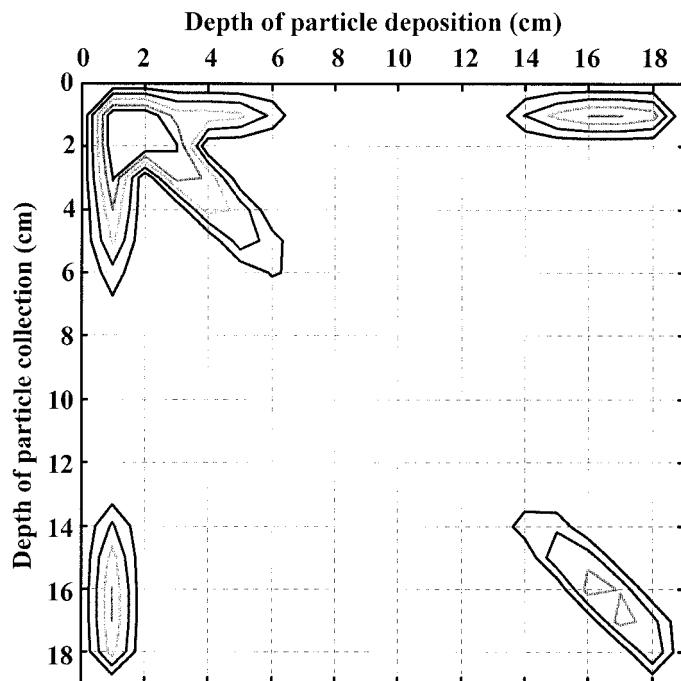
Fig. 8. Diagram of the elasticity matrix. Contours indicate the elements possessing the highest elasticity values. To simplify the display, log(elasticities) are contoured, the box size (Δx) was set at 1 cm, and the model time step (Δt) was set at 1 yr.

position at the sediment surface, and the next largest were associated with surface collection and subsurface deposition at 14–15 cm. The fourth largest group of elasticities was associated with surface sediment collection and egestion at a depth of 3–4 cm.

Discussion

Methods of quantifying bioturbation—Traditionally, bioturbation has been quantified by use of either diffusion or advection models. However, Jumars et al. (1981) modeled sediment transport processes, including selective feeding, as a Markov chain. A transition-matrix model of bioturbation was developed by Foster (1985). This model was extended by Trauth (1998) to examine paleoceanographic time series. Boudreau and Imboden (Boudreau 1986*b*; Boudreau and Imboden 1987) developed a model of bioturbation incorporating an exchange matrix to examine nonlocal mixing phenomena. The transition-matrix model shares many features with these models. In fact, the solids conservation equation (Eq. 2) can be derived from the Boudreau and Imboden model. However, the transition-matrix model possesses a number of features that make it particularly useful for simulating biological reworking mechanisms. Because sediment profile data (both biological and chemical) are usually discrete with respect to depth, it is relatively easy to incorporate these data into the discrete mathematical model. The model possesses simple solutions. A sensitivity analysis can identify the mixing processes that contribute most to the tracer burial rate. Most importantly, mechanisms of particle transport representing the actual depths and rates of movement due to bi-

ological activities or other processes are explicitly included in the model.

There are a number other methods by which biological activities can be quantitatively linked to bioturbation rates. If mixing is quantified by use of a diffusion model, scaling arguments suggest that the biodiffusion coefficient should be proportional to the square of the distance of particle movement divided by the time period between feeding events (Wheatcroft et al. 1990). For communities dominated by conveyor-belt species, the bioadvection rate can be calculated from the product of the volumetric feeding rate and the population density of the dominant deposit feeders. For example, Rice (1986) calculated the sediment bioadvection rate from data on the abundance and feeding rate of *Leitoscoloplos* spp., the most abundant subsurface deposit feeder occupying his study site. By assuming that all sediment mixing was due to deposit feeding by this organism, Rice (1986) was able to accurately predict the vertical profile of the radionuclide tracer [7]Be. One benefit of nonlocal models, including the transition-matrix model proposed here, is the ability to simulate a variety of complex mixing phenomena.

The importance of downward transport in Narragansett Bay—The transition-matrix model was tested by comparison of predicted and measured tracer profiles. The obvious differences between the measured excess ^{210}Pb profile and the ^{210}Pb profile predicted by the model led me to reject the model as initially formulated. These differences indicated that some other mixing mechanism was occurring that was not included in the model. Inclusion of downward transport due to hoeing by the maldanid polychaetes largely resolved the differences between predicted and measured profiles.

This kind of downward transport has been observed by other investigators and may have a variety of important geological, geochemical, and ecological effects. Often termed "sediment subduction," "reverse-conveyor-belt feeding," or "hoeing," it has been observed in a variety of habitats, and many different taxa may be responsible for this process. In shallow water, the maldanid polychaete *Clymenella torquata* was first observed to hoe sediment into its burrow by Dobbs and Whitlatch (1982), who estimated that hoeing accounted for ~3% of the sediment ingested by this species. Myers (1977) observed downward transport of sediment by *P. eximius* and the cirratulid polychaete *Tharyx acutus*. Rice (1986) indicated that the intertidal terrebellid polychaete *Polycirrus medusa* feeds in a similar manner. In deeper water, Wheatcroft et al. (1994) postulated downward transport to explain observed tracer profiles in Massachusetts Bay. Working on the continental slope, Blair et al. (1996) and Levin et al. (1997) observed rapid downward transport of surface sediment and organic matter by polychaetes. Smith et al. (1986) argued that subsurface maxima of tracer profiles in the deep sea were due to downward transport of surface sediment by a sipunculan deposit feeder.

Since this process has been observed at nearly all ocean depths and in many locations, it is not surprising that it was found to be important in determining tracer profiles in Narragansett Bay. However, rates of downward transport are difficult to measure in the laboratory. Also, it is difficult to quantitatively link subsurface peaks in tracer profiles to the

mixing activities of a particular species using traditional bioturbation models. However, I was able to use an inverse approach to calculate the rate of downward particle transport by maldanid polychaetes from the ^{210}Pb profile, because the other mixing rates in the model were independently fixed. The estimate that 40% of sediment ingested by maldanid polychaetes was collected at the sediment surface is >10 times the laboratory estimate of Dobbs and Whitlatch (1982) for the related species *C. torquata.* Yet this high estimate of the maldanid hoeing rate is not unreasonable. There is increasing evidence that these subsurface deposit feeders may collect a high percentage of their food from the sediment surface (Levin et al. 1997). Since the nutritional quality of sediment generally decreases with depth (Rice and Rhoads 1989), there is likely a selective pressure for subsurface deposit feeders to collect and ingest a high percentage of material from the sediment surface.

The hoeing-rate estimate was based on the assumption that individuals hoeing material into their tubes did not select for particles that contained high ^{210}Pb activities. Although recent evidence suggests that hoeing by maldanid polychaetes is not selective (Levin et al. 1997), it is likely that hoeing rates vary temporally. Maldanid polychaetes may respond rapidly to depositional events by collecting and caching recently deposited material such as phytodetritus (Jumars et al. 1990; Levin et al. 1997) rather than previously egested sediment. This would result in the selective mixing of "younger" particles with higher radionuclide activities (Smith et al. 1993). Since phytoplankton can contain high activities of both ^{234}Th and ^{210}Pb (Fisher et al. 1987), intense hoeing after organic matter deposition could select for higher activities of these radionuclides. If particle selection were occurring, this would reduce the mass of sediment required to produce the subsurface maximum of excess ^{210}Pb. However, it would not decrease the importance of surface sediment as food for these deposit feeders.

There are other possible explanations for the subsurface peak in ^{210}Pb activity. Although the filling of abandoned burrows with surface sediment could be occurring at this site, this process is not likely to produce a subsurface peak in tracer activity (Boudreau and Imboden 1987). Another possible explanation for the subsurface peak in ^{210}Pb activity is past deposition of a layer of sediment with low excess ^{210}Pb activity in the depth range between 5 and 15 cm.

I cannot wholly refute this non–steady-state alternative hypothesis by analyzing samples collected on just one date. However, an event that deposited low ^{210}Pb–activity sediment would likely be visible in the profiles of other sediment tracers. Using aluminum as a tracer for crustal material and organic carbon as a tracer for water-column–derived material, I examined the plausibility of this alternative explanation by plotting OC:Al versus depth. The constant decrease in the ratio these elements in the 5- to 15-cm depth range does not support the hypothesis that a change in sediment supply is responsible for the excess ^{210}Pb minimum between 5 and 15 cm. Rather, it is more consistent with relatively constant rate of burial and degradation of organic carbon. The small peak in OC:Al at 15 cm is also consistent with the downward mixing of surface material with higher OC: Al. Although it is possible that a change in sediment supply

would not be reflected in organic carbon and aluminum concentrations, the OC:Al profile is more consistent with the hypothesized steady-state hoeing process than with the alternative explanation of past deposition of a layer of sediment with low excess ^{210}Pb activity.

Hoeing has important ecological consequences. Levin et al. (1997) observed unique assemblages of deposit feeders inhabiting the same depth range as the burrow bottoms of maldanid polychaetes that were hoeing surficial material. This same process may be occurring in Narragansett Bay. The depth distribution of oligochaetes was concentrated in the depth range of 3–4 cm, near the bottom of *P. eximius* tubes and at 14 cm, near the mean depth of the maldanid polychaete tubes.

Mechanisms responsible for determining tracer profiles— After hoeing was included in the model, the measured tracer profiles matched the predicted profiles reasonably well, given the range of variability at the study site. Although it is possible that the model fits were fortuitous, the quantitative agreement between predicted and measured profiles suggests that particle reworking by deposit feeders plus sedimentation are sufficient to determine the depth distributions of excess ^{210}Pb and ^{234}Th at the study site.

The elasticity analysis indicated which mixing processes were most important in determining the overall bioturbation rate. The most important mixing mechanism was upward transport from 2 to 3 cm to the sediment surface. This is the feeding depth range of *N. annulata* and *M. ambiseta.* Although these are small deposit feeders, they were extremely abundant at the study site. The dramatic effects of large numbers of *Nucula* and *Mediomastus* on particle mixing and sediment properties have been observed in the past (Rhoads and Young 1970; Young 1971; Wheatcroft and Martin 1996). The results of the sensitivity analysis quantify the important contribution of these species to the bioturbation rate. The next largest contributor to the overall bioturbation rate was the feeding activity of the maldanid polychaetes (upward and downward transport between 15 cm and the surface), followed by the activities of *P. eximius,* which transported particles from the sediment surface to a depth of 3 cm. Although these species were relatively rare at the study site, their large size resulted in a rapid rate of sediment movement per individual with particle trajectories covering relatively large distances.

The rates of sediment movement by deposit feeders are the key parameters for this model. For the most important species in at the study site, *Nucula* and *Mediomastus,* laboratory ingestion rate data were used to determine particle-transport rates. An inherent assumption was that these laboratory data provided reasonable estimates of ingestion rates in the field. For some of the other species, Cammen's (1980) ingestion-rate model was used. This introduces another source of error into the model. For example, the ingestion rate for a 90-mg deposit feeder feeding on sediment with 2% organic matter predicted by Cammen's model is 510 mg dry sediment d^{-1}. However, the 95% confidence limits range from 130 to just over 2,000 mg dry sediment d^{-1}. Incorporation of this error would likely broaden the range in predicted profiles. Although this source of error is difficult to

include in the transition-matrix model, a more complicated model that includes this variance in deposit-feeding rates could potentially provide more accurate estimates of the error associated with particle-mixing rates.

Future directions and applications of the transition-matrix model

The accuracy of the transition-matrix model is dependent on the quality of data available on deposit-feeding rates and mechanisms. This highlights the need for continued data collection on deposit-feeding rates and mechanisms. These data are particularly scarce for deep-sea taxa. The transition-matrix model can be extended to model the diagenesis of many compounds in addition to radioisotopes. This can be accomplished by replacing the radioactive decay constants in the model with other reaction rate coefficients. In fact, the model could be used to examine the effects of deposit-feeder gut passage on diagenesis by allowing chemical transformations to occur every time sediment is passed trough a gut. Thus, given data on the effects of gut passage on, for example, the degradation of organic matter, the dissolution calcium carbonate, or the solubility of metals or radionuclides, the transition-matrix model could potentially simulate both vertical transport and chemical transformations as a result of deposit feeding and other biological processes.

References

ALLER, R. C. 1982. The effects of macrobenthos on chemical properties of marine sediment and overlying water, p. 53–102. *In* P. L. McCall and M. J. S. Tevesz [eds.], Animal-sediment relations. Plenum.

———, AND J. K. COCHRAN. 1976. ^{234}Th/^{238}U disequilibrium in nearshore sediments: Particle reworking and diagenetic time scales. Earth Planet. Sci. Lett. **29:** 37–50.

BENDER, K., AND W. R. DAVIS. 1984. The effect of feeding by *Yoldia limatula* on bioturbation. Ophelia **23:** 91–100.

BERNER, R. A. 1980. Early diagenesis: A theoretical approach. Princeton Univ. Press.

BLAIR, N. E., L. A. LEVIN, D. J. DEMASTER, AND G. PLAIA. 1996. The short-term fate of fresh algal carbon in continental slope sediments. Limnol. Oceanogr. **41:** 1,208–1,219.

BOUDREAU, B. P. 1986*a*. Mathematics of tracer mixing in marine sediments: I. Spatially dependent, diffusive mixing. Am. J. Sci. **286:** 161–198.

———. 1986*b*. Mathematics of tracer mixing in marine sediments: II. Nonlocal mixing and biological conveyor-belt phenomena. Am. J. Sci. **286:** 199–238.

———. 1997. Diagenetic models and their implementation. Springer-Verlag.

———, AND D. M. IMBODEN. 1987. Mathematics of tracer mixing in marine sediments: III. The theory of nonlocal mixing within sediments. Am. J. Sci. **287:** 693–719.

CAMMEN, L. M. 1980. Ingestion rate: An empirical model for aquatic deposit feeders and detritivores. Oecologia **44:** 303–310.

CASWELL, H. 1978. A general formula for the sensitivity of population growth rate to changes in life history parameters. Theor. Pop. Biol. **14:** 215–230.

———. 1989. Matrix population models: Construction, analysis, and interpretation. Sinauer.

CHRISTMAN, R. F., AND E. T. GJESSING. 1983. Aquatic and terrestrial humic materials. Ann Arbor Science.

DOBBS, F. C. 1981. Community ecology of a shallow subtidal sand flat with emphasis on sediment reworking by *Clymenella torquata.* M.S. thesis, Univ. of Connecticut.

———, AND R. B. WHITLATCH. 1982. Aspects of deposit feeding by the polychaete *Clymenella torquata.* Ophelia **21:** 159–166.

FISHER, N. S., J.-L. TEYESSIE, S. KRISHNASWAMI, AND M. BASKARAN. 1987. Assimilation of Th, Pb, U, and Ra in marine phytoplankton and its geochemical significance. Limnol. Oceanogr. **32:** 131–142.

FOSTER, D. W. 1985. BIOTURB: A Fortran program to simulate the effects of bioturbation on the vertical distribution of sediment. Comput. Geosci. **11:** 39–54.

GERINO, M., R. C. ALLER, C. LEE, J. K. COCHRAN, J. Y. ALLER, M. A. GREEN, AND D. HIRSCHBERG. 1998. Comparison of different tracers and methods used to quantify biourbation during a spring bloom: ^{234}Thorium, luminophores and chlorophyll *a*. Estuar. Coast. Shelf Sci. **46:** 531–547.

GOLDBERG, E. D., AND M. KOIDE. 1962. Geochronological studies of deep-sea sediments by the ionium-thorium method. Geochim. Cosmochim. Acta. **26:** 417–450.

GRASSLE, J. F., J. P. GRASSLE, L. S. BROWN-LEGER, R. F. PETRECCA, AND N. J. COPLEY. 1985. Subtidal macrobenthos of Narragansett Bay. Field and mesocosm studies of the effects of eutrophication and organic input on benthic populations, p. 421–434. *In* J. S. Gray and M. E. Christiansen [eds.], Marine biology of polar regions and effects of stress on marine organisms. Wiley.

GUINASSO, N. L., AND D. R. SCHINK. 1975. Quantitative estimates of biological mixing rates in abyssal sediments. J. Geophys. Res. **80:** 3,032–3,045.

HEDGES, J. I., AND J. H. STERN. 1984. Carbon and nitrogen determinations of carbonate-containing solids. Limnol. Oceanogr. **29:** 657–663.

HUGHES, J. E. 1996. Size-dependent small-scale dispersion of the capitellid polychaete, *Mediomastus ambiseta.* J. Mar. Res. **54:** 915–937.

JUMARS, P. A., L. M. MAYER, J. W. DEMING, J. A. BAROSS, AND R. A. WHEATCROFT. 1990. Deep-sea deposit-feeding strategies suggested by environmental and feeding constraints. Philos. Trans. R. Soc. Lond. A Math. Phys. Sci. **331:** 85–101.

———, A. R. M. NOWELL, AND R. F. L. SELF. 1981. A simple model of flow-sediment-organism interaction. Mar. Geol. **42:** 155–172.

KEMENY, J. G., AND J. L. SNELL. 1976. Finite Markov chains, 2nd ed. Van Nostrand Reinhold.

KREMER, J. N., AND S. W. NIXON. 1978. A coastal marine ecosystem. Springer-Verlag.

LAMOTHE, P. J., T. L. FRIES, AND J. J. CONSUL. 1986. Evaluation of a microwave oven system for the dissolution of geologic samples. Anal. Chem. **58:** 1,881–1,886.

LEVIN, L., N. BLAIR, D. DEMASTER, G. PLAIA, W. FORNES, C. MARTIN, AND C. THOMAS. 1997. Rapid subduction of organic matter by maldanid polychaetes on the North Carolina slope. J. Mar. Res. **55:** 595–611.

LOPEZ, G. R., AND I.-J. CHENG. 1983. Synoptic measurements of ingestion rate, ingestion selectivity, and absorption efficiency of natural foods in the deposit-feeding molluscs *Nucula annulata* (Bivalvia) and *Hydrobia totteni* (Gastropoda). Mar. Ecol. Prog. Ser. **11:** 55–62.

———, G. L. TAGHON, AND J. S. LEVINTON. 1989. The ecology of marine deposit feeders. Springer-Verlag.

MCCAFFREY, R. J., AND OTHERS. 1980. The relation between pore water chemistry and benthic fluxes of nutrients and manganese in Narragansett Bay, Rhode Island. Limnol. Oceanogr. **25:** 31–44.

MYERS, A. C. 1977. Sediment processing in a marine subtidal sandy

bottom community. I. Physical aspects. J. Mar. Res. **35:** 609–632.

NOZAKI, Y., J. K. COCHRAN, K. K. TUREKIAN, AND G. KELLER. 1977. Radiocarbon and ^{210}Pb distribution in submersible-taken deep-sea cores from project FAMOUS. Earth Planet. Sci. Lett. **34:** 167–173.

OFFICER, C. B., AND D. R. LYNCH. 1983. Determination of mixing parameters from tracer distributions in deep-sea sediment cores. Mar. Geol. **52:** 59–74.

OLSEN, C. R., N. H. CUTSHALL, AND I. L. LARSEN. 1982. Pollutant-particle associations and dynamics in coastal marine environments: A review. Mar. Chem. **11:** 501–533.

POPE, R. H., D. J. DEMASTER, C. R. SMITH, AND H. SELTMANN, JR. 1996. Rapid bioturbation in equatorial Pacific sediments: Evidence from excess [234]Th measurements. Deep-Sea Res. II **43:** 1,339–1,364.

RHOADS, D. C., AND D. K. YOUNG. 1970. The influence of deposit-feeding organisms on sediment stability and community structure. J. Mar. Res. **28:** 150–178.

RICHTER, R. 1952. Sediment-Gaseinien und Sedifluktion uberhaupt: Notizbl. Hess. L.-Amt. Bodenforsch **3:** 67–81.

RICE, D. L. 1986. Early diagenesis in bioadvective sediments: Relationships between the diagenesis of beryllium-7, sediment reworking rates, and the abundance of conveyor-belt feeders. J. Mar. Res. **44:** 149–184.

———, AND D. C. RHOADS. 1989. Early diagenesis of organic matter and the nutritional value of sediment. *In* G. Lopez, G. L. Taghon, and J. S. Levinton [eds.], The ecology of marine deposit feeders. Springer-Verlag.

ROBBINS, J. A. 1986. A model for particle-selective transport of tracers in sediments with conveyor belt deposit feeders. J. Geophys. Res. **91:** 8,542–8,558.

SHULL, D. H. 2000. Mechanistic modeling of particle mixing in marine sediments. Ph.D. thesis, Univ. of Massachusetts.

ROBERTS, F. S. 1976. Discrete mathematical models. Prentice-Hall.

SMITH, C. R., R. H. POPE, D. J. DEMASTER, AND L. MAGAARD. 1993. Age-dependent mixing of deep-sea sediments. Geochim. Cosmochim. Acta. **57:** 1,473–1,488.

SMITH, J. N., B. P. BOUDREAU, AND V. NOSHKIN. 1986. Plutonium and ^{210}Pb distributions in northeast Atlantic sediments: Subsurface anomalies caused by non-local mixing. Earth. Planet. Sci. Lett. **81:** 15–28.

SUN, M.-Y., R. C. ALLER, AND C. LEE. 1991. Early diagenesis of chlorophyll-*a* in Long Island Sound sediments: A measure of carbon flux and particle reworking. J. Mar. Res. **49:** 379–401.

THAYER, C. W. 1983. Sediment-mediated disturbance and the evolution of marine benthos, p. 480–595. *In* M. J. S. Tevesz and P. L. McCall [eds.], Biotic interactions in recent and fossil benthic communities. Plenum.

TRAUTH, M. H. 1998. TURBO: A dynamic-probabilistic simulation to study the effects of bioturbation on paleoceanographic time series. Comput. Geosci. **24:** 433–441.

WHEATCROFT, R. A. 1991. Conservative tracer study of horizontal sediment mixing rates in a bathyal basin, California borderland. J. Mar. Res. **49:** 565–588.

———. 1992. Experimental tests for particle size-dependent bioturbation in the deep ocean. Limnol. Oceanogr. **37:** 90–104.

———, P. A. JUMARS, C. R. SMITH, AND A. R. M. NOWELL. 1990. A mechanistic view of the particulate biodiffusion coefficient: Step lengths, rest periods and transport directions. J. Mar. Res. **48:** 177–207.

———, AND W. R. MARTIN. 1996. Spatial variation in short-term ([234]Th) sediment bioturbation intensity along an organic-carbon gradient. J. Mar. Res. **54:** 763–792.

———, I. OLMEZ, AND F. X. PINK. 1994. Particle bioturbation in Massachusetts Bay: Preliminary results from a new technique. J. Mar. Res. **52:** 1,129–1,150.

———, V. R. STACZAK, AND C. A. BUTMAN. 1998. The impact of population abundance on deposit-feeding rate of a cosmopolitan polychaete worm. Limnol. Oceanogr. **43:** 1,948–1,953.

YOUNG, D. K. 1971. Effects of infauna on the sediment and seston of a subtidal environment. Vie Milieu (Suppl.) **22:** 557–571.